Available online at www.sciencedirect.com
SCIENCE DIRECT®
PERGAMON
Radiation Physics and Chemistry 68 (2003) 757–764
Radiation Physics and Chemistry
www.elsevier.com/locate/radphyschem

Technical note

Measurement of photon mass–energy absorption coefficients of paraffin wax and gypsum at 662 keV

Bassam Z. Shakhreet[a], C.S. Chong[a], T. Bandyopadhyay[b], D.A. Bradley[c], A.A. Tajuddin[a], A. Shukri[a,*]

[a] School of Physics, Universiti Sains Malaysia, 11800 Penang, Malaysia
[b] Variable Energy Cyclotron Center, Calcutta, India
[c] School of Physics, University of Exeter, Exeter, UK

Received 23 August 2001; accepted 20 February 2003

Abstract

One of the most important gamma radiation quantities with respect to radiation dosimetry and health physics applications is mass–energy absorption. Direct measurements of the coefficient of mass–energy absorption, μ_{en}/ρ, are difficult and typically recourse is taken to theoretical computations. In this study, we have determined μ_{en}/ρ experimentally using a simple and direct method based on paraxial sphere transmission, using a proportional response gamma detector. The effects of nonparaxiality and of finite sample thickness have been accounted for, using extrapolation procedures. The deviation from nonproportionality and other corrections have been shown to be small.

For 662 keV photons, the measured value of μ_{en}/ρ for paraffin wax has been determined using the above method as $(3.37 \pm 0.05) \times 10^{-3}\,m^2/kg$. This compares favourably with the theoretically computed value of $3.35 \times 10^{-3}\,m^2/kg$ given by Hubbell and Seltzer (1997). The measured value of μ_{en}/ρ for gypsum has been determined as $(2.96 \pm 0.01) \times 10^{-3}\,m^2/kg$, which also compares favourably with the theoretically computed value of $2.99 \times 10^{-3}\,m^2/kg$ given by Hubbell and Seltzer (1997).

Comparison of measurements made using spherical shells and cylindrical shells has been provided with the intent of determining the equivalence of these two phantom shapes. In addition to the question of sensitivity of measurements to shell thickness, the investigation also examined the dependency of measured values on source-to-detector separation. Results obtained for the two shapes show close agreement with regard to the values of μ_{en}/ρ obtained using either shape.

1. Introduction

The coefficient of photon interaction most appropriate to radiation dosimetry is that of mass–energy absorption (μ_{en}/ρ). The coefficient μ_{en}/ρ refers to the amount of energy dissipated by secondary electrons set in motion as a result of interactions between incident photons and matter. Under conditions of charged particle equilibrium, the energy dissipated by an electron in the given volume can be equated to the energy absorbed in that volume.

Direct, accurate measurements of μ_{en}/ρ are difficult. Evaluation by calorimetric measurements, yielding temperature changes of the order of a milli-Kelvin or less are typically limited to standardizing laboratories. However, one other possibility for direct evaluation of μ_{en}/ρ is through energy-proportional detection of unmodified and modified photon spectra, the measured transmission factors being directly related to energy absorption. Earlier measurements were exclusively made using spherical shells of low atomic number media (Bradley et al., 1989). A particular problem relates to the shape and thickness of an absorber; symmetry indicates use of spherical absorbers, while physical constraints further indicate the use of thin shells (generally being of

*Corresponding author.
E-mail address: ashukri@usm.my (A. Shukri).

0969-806X/03/$ - see front matter
doi:10.1016/S0969-806X(03)00327-X

thickness less than one mean-free path). Greater utility of the method would seem to suggest the formulation of more easily fabricated shapes, offering equivalence of response.

The present investigation compares the response of spherical absorbers with that of cylindrical absorbers and also looks at the question of sensitivity of measurements to shell thickness. Measurements have been made on spheres and cylinders of paraffin wax ($C_{16}H_{34}$) and gypsum ($CaSO_4 \cdot 2H_2O$) for the photon energy 662 keV. Since the method is only strictly valid for point sources and point detectors, the present investigation also examines the dependency of measured values on source-to-detector separation.

2. Materials and methods

2.1. Methodology

The most basic requirement of the method used herein is for energy-proportional detection. A detector whose efficiency is proportional to energy is useful for measurement of energy flux and energy dosimetry, etc. The proportional response detector used in the present study is based on a 5 cm × 5 cm NaI (Tl) scintillation detector, prefaced by a paraxial mounted aluminum filter. This setup is based on the results of work done by Achmad and Ghose (1982), who developed a simple proportional energy response detector using an NaI (Tl) detector prefaced by an axially placed filter of suitable material of appropriate thickness.

The overall efficiency (ε_j), for paraxially incident photons of energy E_j, of a system of filters placed coaxially with respect to NaI (Tl) detector, is given by

$$\varepsilon_j = \varepsilon_{0j}[1 - \sum_i f_i + \sum_i f_i \exp(-\mu_{ij} t_i)], \tag{1.1}$$

where t_i is the axial length of the ith filter, μ_{ij} is the total absorption (or attenuation) coefficient of the material of the ith filter for photons of energy E_j and f_i is the fraction of time that the ith filter is present before the scintillator. Where a simple system consisting of a single filter is considered, Eq. (1.1) becomes

$$\varepsilon_j = \varepsilon_{0j}[(1-f) + f \exp(-\mu_{jt})], \tag{1.2}$$

where μ is a constant and hence, in the ε vs. f diagram, ε is a linear function of f, with an intercept ($\varepsilon = \varepsilon_0$) on the ε-axis ($f = 0$) and an intercept equal to ($\varepsilon' = \varepsilon_0 e^{-\mu t}$) on the f-axis ($f = 1$). This is shown in Fig. 1 for a 5.08 cm thick NaI (Tl) and an aluminum filter of areal density 20 g/cm^2 for various photon energies (Ghose, 1987). It can be seen that the lines drawn for different energies intersect with each other within a small region of f.

For proportional response counters, the efficiency of the detector system, is given, as before, by

$$\varepsilon_j = kE_j = [(1-f) + f \exp(-\mu_j t)]\varepsilon_{0j}, \tag{1.3}$$

$$E_j/\varepsilon_{0j} = [(f/k)\exp(-\mu_j t)] + [(1-f)/k], \tag{1.4}$$

$$E_j/\varepsilon_{0j} = m \exp(-\mu_j t) + c, \tag{1.5}$$

where $m = f/k$ and $c = (1-f)/k$, so that $m + c = 1/k$.

Thus,

$$-\mathrm{d}/\mathrm{d}\mu_j(E_j/\varepsilon_{0j}) = mt \exp(-\mu_j t) \tag{1.6}$$

and

$$\ln[-\mathrm{d}/\mathrm{d}\mu_j(E_j/\varepsilon_{0j})] = \ln(mt) - \mu_j t. \tag{1.7}$$

We note, that for a single filter used continuously, we have for proportional response counters:

$$k(E_j/\varepsilon_{0j}) = \exp(-\mu_j t), \tag{1.8}$$

k being a constant. Ideally, we have, by taking logarithms on both sides and forming differences,

$$\ln \delta(E_j/\varepsilon_{0j}) = -t\, \delta(\mu_j), \tag{1.9}$$

where δ represents changes in the quantity in the parenthesis. Hence,

$$t = -\ln \delta(E_j/\varepsilon_{0j})/\delta(\mu_j). \tag{1.10}$$

From Eq. (1.10) it is an expectation that the quantity $\ln(E_j/\varepsilon_{0j})$, which depends on the characteristics of the detector, should vary linearly with μ_j. Linearity is indicated to be valid for low Z materials like carbon, paraffin, and aluminum for gamma rays above 40 keV. Materials with moderately large Z are found to be unsuitable as filter material, especially if low-energy photons are present in the gamma ray spectrum under measurement.

For a 2 in (5.08 cm) NaI (Tl) detector, Achmad and Ghose (1982) found using an algebraic method that $t = 20.0$ g/cm^2 of aluminum forms a suitable filter. The value of f necessary for this case was found to be 0.770. The intrinsic paraxial efficiency ε_o of an NaI (Tl) scintillator at 0.662 MeV is about 0.77 and the overall efficiency ε is 0.302 (Achmad and Ghose, 1982). The value of μ for aluminum at 0.662 MeV is about 0.0770 cm^2/g.

Geometrical requirements call for an absorbing shell, enclosing, and concentric with the photon source. Source dimensions should also be small compared to the source-to-detector separation in order to provide approximation to a point source and detector situation. Detector collimation ensures the sampling of a constant fraction of the incident beam.

Physical requirements call for a thickness of absorbing shell sufficient for the occurrence of a statistically significant number of interactions with minimal occurrence of multiple scattering. Surrounding structures should

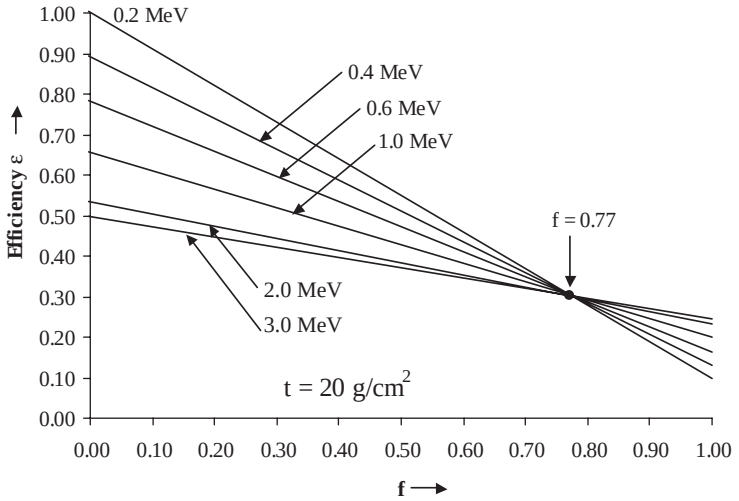

Fig. 1. Geometrical method for finding the value of the factor f (see text for details of this) for an aluminum filter of thickness t, to be used with a 5.08 cm thick NaI (Tl) crystal (Ghose, 1987).

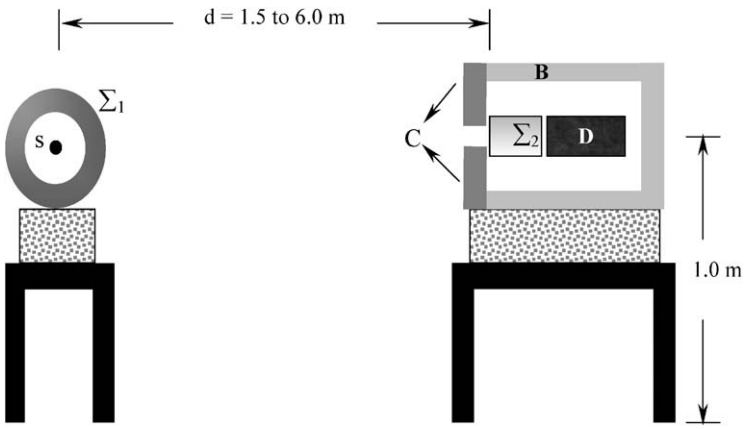

Fig. 2. Schematic presentation of the experimental arrangement used in measuring μ_{en}/ρ for paraffin wax; S denotes the photon source, Σ_1 the wax spherical absorbing shell, Σ_2 the aluminum filter, C the detector collimation, D the NaI detector and B the cylindrical Pb shields. A similar arrangement was employed for cylindrical absorbing shells.

also be sufficiently distant so that source-dependent backgrounds remain a small fraction of the signal.

A particularly important measurement concerns the bare detector response to a bare source. Care has been taken to subtract the below Compton-edge bare-detector response from all data runs involving absorbing shells.

Fig. 2 illustrates the essential features of the setup. The detector is placed far enough from the attenuating layers so that any particle that is deflected in an interaction will miss the detector. The beam is collimated to be just large enough to cover the detector uniformly, thereby minimizing the number of scattered or secondary particles (Compton, fluorescence, Bremsstrahlung) generated in the attenuator. The radiation beam source is located in the centre of the attenuator so that the attenuator will be itself the radiation source with a homogenous shape. Moreover, the intensity of the primary beam at the detector will then be nearly independent of distance from the attenuator, while the intensity of the scattered and secondary particles will decrease as the inverse square of that distance. Thus, the relative strength of the primary beam increases with detector distance, allowing reduction of the nonprimary radiation to a negligible level at the detector.

In an ideal sphere transmission geometry, we use a point source emitting n_o photons (each of energy E_0) per second, surrounded by an infinitesimally thin absorber $\sum$ (thickness dx), while the detector D accepts paraxially incident photons emitted within a constant fraction of the available solid angle (Ghose, 1965). The fraction of photons absorbed and scattered by $\sum$ is

$\mu_a\,dx$ and $\mu_s\,dx$, respectively, where μ_a is the linear absorption and μ_s is the linear scattering coefficient of $\sum$ for photons of energy E_0. If the detector is of the proportional-response type, the efficiency is given by

$$\varepsilon(E) \propto E,$$

$$\varepsilon(E) = kE, \tag{2.1}$$

where k is independent of E. The counting rate in the absence of the absorber is then

$$I_0 = kn_0E_0, \tag{2.2}$$

where, in general,

$$I = n\varepsilon(E).$$

Further, the change in counting rate with $\sum$ is given by

$$I = n\varepsilon = nkE \Rightarrow dI = k\,\Delta E\,dn.$$

Since $dn = -\mu n_0\,dx$, then

$$\begin{aligned} dI &= -k\,\Delta E\mu n_0\,dx \Rightarrow dI = -kn_0\,dx(\mu\,\Delta E),\\ dI &= kn_0\,dx[-\mu(E_0 - E_s)]\\ &= kn0\,dx[-(\mu_a + \mu_s)E_0 + \mu_sE_s],\\ dI &= n_0k\,dx[-(\mu_a + \mu_s)E_0 + \mu_s\int f(E)E\,dE]. \end{aligned} \tag{2.3}$$

The integral in the above equation, which extends over the entire primary scattered photon spectrum, measures the contribution of the scattered photons to the counting rate, $f(E)\,dE$, this being the normalized spectral distribution of the scattered photons. Thus,

$$\frac{dI}{I_0} = -\left\{\mu_a + \mu_s\left[1 - \frac{\int f(E)E\,dE}{E_0}\right]\right\}dx. \tag{2.4}$$

In Eq. (2.4), the quantity within the inner brackets represents the fraction of incident photon energy that is absorbed through scattering processes, assuming that tertiary and higher-order photons arising, for example, from the Bremsstrahlung of photoelectrons, are not detected by detector. Under this assumption, we can write

$$\frac{dI}{I_0} = -\mu_{en}\,dx = -\left(\frac{\mu_{en}}{\rho}\right)\rho\,dx. \tag{2.5}$$

For a finite but small absorber thickness, the above derivation holds well when multiple interactions can be neglected, such that one then obtains

$$I = I_0\exp\left[\left(-\frac{\mu_{en}}{\rho}\right)\rho x\right], \tag{2.6}$$

where ρ is the physical density of the absorbing medium and x is the radial thickness of the shell.

Measurement of the transmission factor $T = I/I_0$ leads to direct evaluation of the mass–energy absorption coefficient.

2.2. Spherical-shell absorbers

The arrangement of Fig. 2, used in evaluations of μ_{en}/ρ, is similar to that used in earlier investigations by this group (Bradley et al., 1989). Paraffin wax and gypsum spheres were fabricated in the form of shells having inner diameters 5.0–14.0 cm, each with outer diameter 30.0 cm. Each sphere was constructed from matching hemispheres and each assembly was provided with a single 1.0 cm diameter channel to allow introduction and withdrawal of the source mounted on the tip of a thin rigid wire. Random rotations performed around several axes of the sphere have shown that the hemispherical interface and 1.0 cm borehole produce immeasurable effect on transmission values.

Radial thicknesses of shells were chosen to have values of less than two mean free paths. Measurements of transmission were carried out for various separations of source and detector, over the range 1.5–6.0 m. Lateral alignment of the assembly was obtained to within a precision of 3 mm using a cathetometer. Photon spectra were recorded using a multi-channel analyser and associated electronics, whilst energy proportionality was achieved using a cylindrical aluminum filter, 7.0 cm diameter and 7.5 cm in length.

In the present study, a 3 mm diameter ^{137}Cs bead (662 keV primary gamma photon energy) of nominal activity 7.4 GBq has been used. Counting times were different for each distance but were kept the same for equal distances. Room-scattering corrections to the counting rates were necessary; count rates obtained with a Pb shadow bar in place between the source and detector were subtracted to offset the source-dependent background.

2.3. Cylindrical shell absorbers

Each cylindrical shell was constructed from a stacked pair of equisized solid paraffin wax or gypsum cylinders to form an absorber of outer diameter 25 cm and height 14 cm (providing, to within 10%, the same weight of paraffin wax or gypsum as corresponding spheres). The cylinders were machined to provide inner diameters ranging from 5–14 cm with again a 1.0 cm diameter channel provided to allow the source to be introduced into the interior of the cylinder. The cylindrical shells were placed in the same position as the spheres, but with the cylindrical axis perpendicular to the source–detector axis.

Counting times were again different for each distance but were kept the same for the spherical and cylindrical scattering shells, source to detector separations being in the range 1.5–6.0 m. Room-scattering corrections were again required.

3. Results and discussion

Account has been made of modifications to the broadly two-component spectrum comprising the full-energy peak area (FEA) and a degraded energy region (DER), in accord with the following situations.

1. Bare detector response to a monoenergetic source of photons. Here the counting rate was measured in the absence of the absorber (I_0).
2. Introduction of an aluminum filter prefacing the detector. This was performed to convert the detector to a proportional response type detector.
3. Introduction of an absorbing shell surrounding the source. In this arrangement, the counting rate with the absorber (I) was measured.

The results shown in Figs. 3 and 4 are for spheres of paraffin wax and gypsum, respectively, each with a wall thickness of 10 cm. For regions beyond $D = 3.0$ m, both figures reveal highly linear variation of integrated counting rate (with a correlation coefficient of $r = +0.994$ for the paraffin wax sphere degraded energy region and $r = +0.995$ for the gypsum sphere degraded energy region), for each of the two components of the spectrum, as a function of the inverse square of source–detector separation. This behavior was also found valid for all other spherical and cylindrical shell dimensions. Integration was carried out for all photon energies $E \geqslant 100$ keV (to exclude noise) up to and including the full-energy peak area.

Overall uncertainty in the measured value of μ_{en}/ρ, including statistical uncertainty, positional errors, omission of inclusion of photon energies of less than 100 keV and departures from ideal linearity of the detector, are estimated to be less than 3%. The measured value of μ_{en}/ρ for paraffin wax is found to be within 3% of the value $3.37 \times 10^{-3}\,m^2\,kg^{-1}$ interpolated from the tabulations of Hubbell and Seltzer (1997).

The results for paraffin wax and gypsum cylinders of wall thickness 10 cm are shown in Figs. 5 and 6, respectively. From these, it is apparent that there exists a systematic trend for overestimating μ_{en}/ρ for small source-to-detector separations, the paraxial approximation being poor at these distances. Marginal photons emanating from the sphere traverse oblique paths in the filter and are therefore less efficiently detected than central rays, resulting in larger cross sections than corresponding predictions. Conversely, it is apparent that linearity has been satisfied for large source-to-detector separations, indicating that the point source approximation is valid for sufficiently large distances from the phantom.

Figs. 7 and 8, for paraffin wax and gypsum cylinders and spheres, respectively, show the variation of integrated counting rates with shell thickness for the full-energy peak area of the two spectral regions and

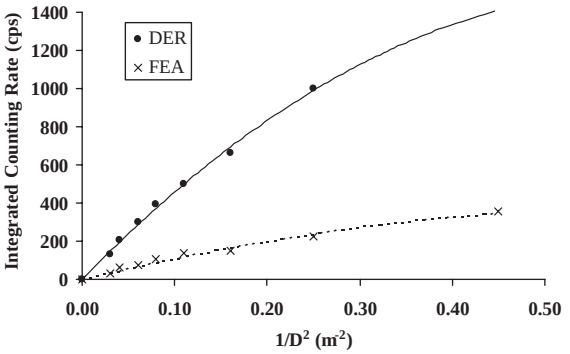

Fig. 3. Integrated counting rate vs. inverse square of source–detector distance (for paraffin sphere with shell thickness 10.0 cm). In Figs. 3–8, FEA is the full-energy peak area, and DER is the degraded energy region.

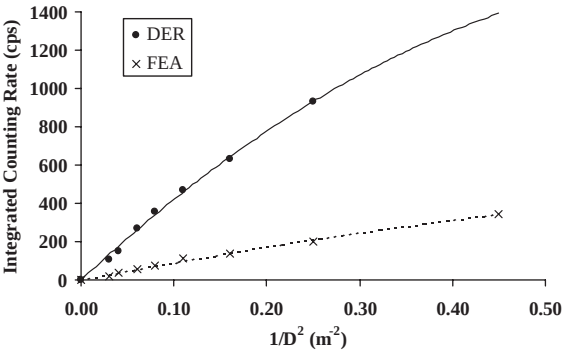

Fig. 4. Integrated counting rate vs. inverse square of source–detector distance (for gypsum sphere with shell thickness 10.0 cm).

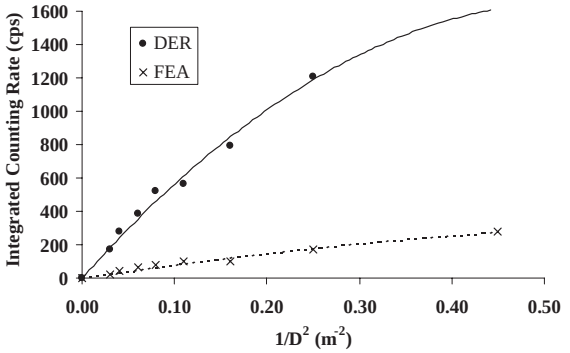

Fig. 5. Integrated counting rate vs. inverse square of source–detector distance (for paraffin cylinder with shell thickness 10.0 cm).

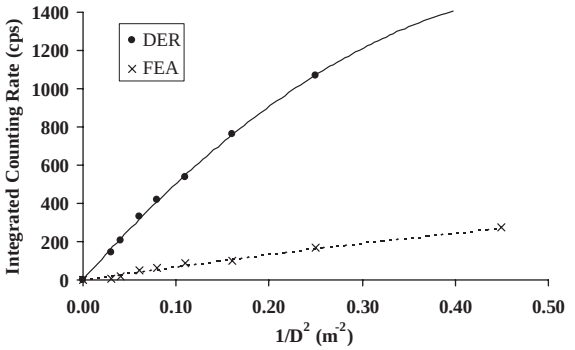

Fig. 6. Integrated counting rate vs. inverse square of source–detector distance (for gypsum cylinder with shell thickness 10.0 cm).

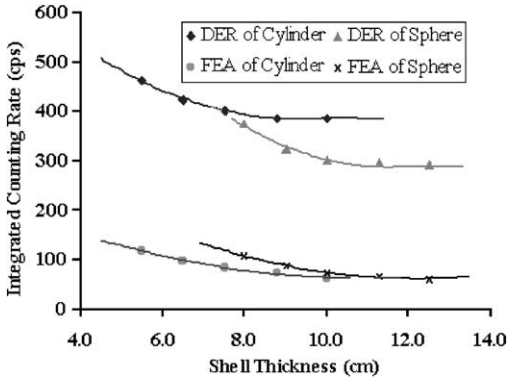

Fig. 7. Integrated counting rate as a function of paraffin wax shell thickness at a fixed source–detector distance of 4.0 m.

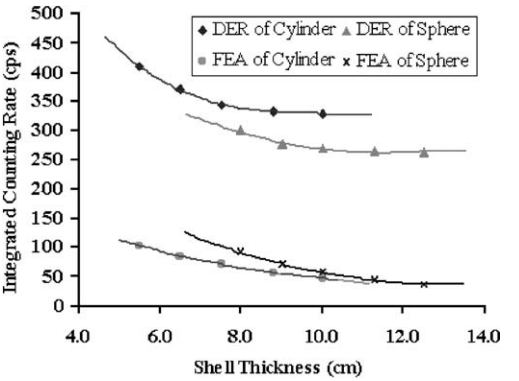

Fig. 8. Integrated counting rate as a function of gypsum shell thickness at a fixed source–detector distance of 4.0 m.

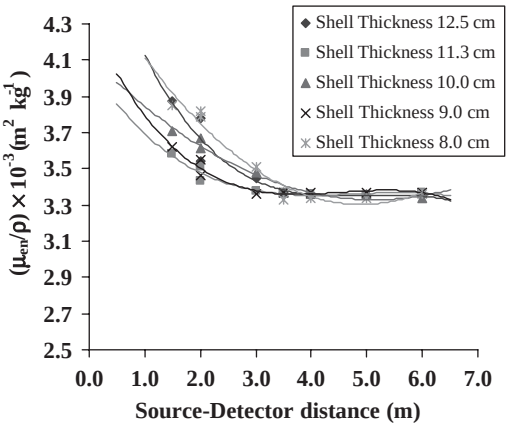

Fig. 9. Variation in apparent values of μ_{en}/ρ as a function of source–detector separation (for paraffin wax sphere).

degraded energy region, at the particular source–detector distance of 4.0 m. With reduction in shell thickness, transmission increases in accordance with reduction in absorption and scattering. Approximate compensation between absorption and scattering is also apparent. Data for thinner spherical shells are not currently available as problems of fabrication occur; similar features are nevertheless to be anticipated.

While integrated counting rates for the degraded spectral region are higher for cylindrical than spherical shells, the converse is observed for photopeak intensity data; the inexact compensatory effect noted earlier translates to corresponding responses that are approximately equal to within 10%. The result tends to suggest that the mass of an absorber plays a dominating role over details of absorber geometry for approximately paraxial geometries. The present method indicates that directly evaluating μ_{en}/ρ by using cylindrical absorbing shells provides close approximation to spherical shells. If we assume the null hypothesis, H_0, that *there is no difference in the value of* μ_{en}/ρ *for sphere and cylinder*, then the following statistics result. The *t*-statistic is equal to 0.610 and 0.880 for the paraffin wax and gypsum (cylinders and spheres) respectively. Now, Degree of freedom (DF) = Number of pairs − 1 and since there are 40 pairs of sphere and cylinder values for each material, DF = 39. From the tables of the value of *t*-statistic, for DF = 39 and $P = 0.03$, the *t*-statistic is 2.252. Since the *t*-statistic for both cases is less than 2.252, we cannot reject the null hypothesis H_0 at the 0.03 level of significance. We can conclude that there is no detectable difference, at this level of significance, in the values of μ_{en}/ρ obtained for the spherical and cylindrical shells.

Figs. 9 and 10 provide data for the range of paraffin wax spheres and cylinders, respectively, while Figs. 11 and 12 are those for gypsum spheres and cylinders, respectively. These graphs show the variation of the apparent value of μ_{en}/ρ, as a function of the source–detector separation. It can be seen that beyond about 3.0 m, effects of nonparaxiality are not appreciable within the limits set by experimental errors. It has also been found that the value of μ_{en}/ρ is somewhat

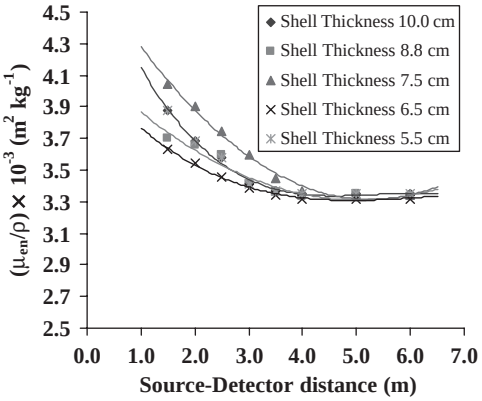

Fig. 10. Variation in apparent values of μ_{en}/ρ as a function of source–detector separation (for paraffin wax cylinder).

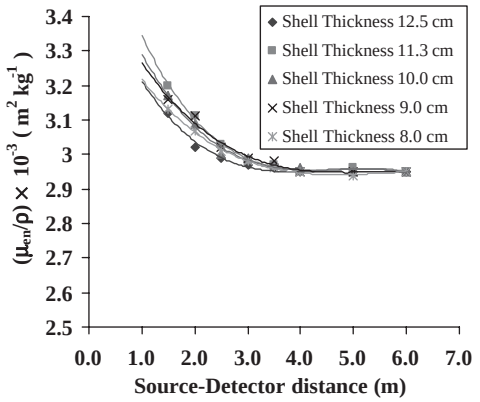

Fig. 11. Variation in apparent values of μ_{en}/ρ as a function of source–detector separation (for gypsum sphere).

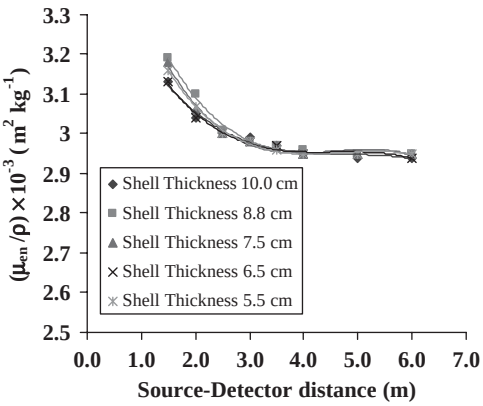

Fig. 12. Variation in apparent values of μ_{en}/ρ as a function of source–detector separation (for gypsum cylinder).

insensitive to the thickness of the absorber. This is not surprising given that μ_{en}/ρ is only weakly dependent on the energy of photons in the energy range under consideration.

4. Summary and conclusion

The method already described in an earlier paper (Bradley et al., 1989) is based on paraxial sphere transmission using a proportional-response gamma detector. A particular problem relates to the shape and thickness of an absorber; symmetry indicates use of spherical absorbers. Greater utility of this method suggests the formulation of more easily fabricated shapes (in particular cylinders) offering equivalence of response.

Measurements using spherical shells of low atomic number media were compared with those using cylindrical shells. The equivalence of these two phantom shapes is seen to exist, the results obtained for the two shapes showing close comparability between values of (μ_{en}/ρ) obtained using either shape. As a result, the cylinder is recommended for use in further studies of (μ_{en}/ρ).

From our investigations, it can be concluded that linearity has been satisfied for large ($\geqslant 3.0$ m) source-to-detector separations, indicating the point source approximation to be valid for sufficiently large distances from the phantom.

Integrated counting rates for the degraded spectral region were higher for the cylindrical shells when compared with comparable thickness spherical shells, the converse being observed for photopeak intensity data. The mass of an absorber appears to play the dominating role over details of absorber geometry for approximately paraxial geometries.

The value of μ_{en}/ρ is found to be relatively insensitive to the thickness of the absorber. This is not surprising given that μ_{en}/ρ is only weakly dependent on the energy of photons in the energy range under consideration.

Excellent agreement between the measured values and the theoretical values of μ_{en}/ρ for paraffin wax and gypsum has been obtained. Specifically, the measured values of μ_{en}/ρ for paraffin wax and gypsum were found to be within 3% of the respective values 3.37×10^{-3} and $2.96 \times 10^{-3}\,m^2\,kg^{-1}$, interpolated from the tabulations of Hubbell and Seltzer (1997).

Acknowledgements

The authors are grateful to Universiti Sains Malaysia and the University of Exeter for support of this work. Many thanks also go to Mr. Burhanudin Wahi and Mr. Azmi Omar for their technical assistance.

References

Achmad, A., Ghose, A.M., 1982. Proportional response detector systems. Proceedings of the Second International Symposium on Radiation Physics, USM, Penang, p. 370.

Bradley, D.A., Chong, C.S., Shukri, A., Tajuddin, A.A., Ghose, A.M., 1989. A new method for the direct measurement of the energy absorption coefficient of gamma rays. Nucl. Instrum. Methods A 280, 392–394.

Ghose, A.M., 1965. Sphere transmission method for the measurement of atomic photoelectronic cross-sections. Nucl. Instrum. Methods 34, 45–53.

Ghose, A.M., 1987. Optimization and Symmetry in Experimental Radiation Physics. EU Joint Research Centre, Ispra, CEC Report EUR 10968 (Luxembourg).

Hubbell, J.H., Seltzer, S.M., 1997. Tables of X-ray Mass Attenuation Coefficients and Mass Energy-Absorption Coefficients (version 1.03) (online). Available: http://physics.nist.gov/xaamdi. National Institute of Standards and Technology, Gaithersburg, MD. Originally published as NISTIR 5632, National Institute of Standards and Technology, Gaithersburg, MD.